The case for dynamical dark energy revisited

Ujjaini Alam[a], **Varun Sahni**[a] **and A. A. Starobinsky**[b]

[a] Inter-University Centre for Astronomy & Astrophysics, Puné 411 007, India
[b] Landau Institute for Theoretical Physics, 119334 Moscow, Russia

Abstract. We investigate the behaviour of dark energy using the recently released supernova data of Riess et al., 2004 and a model independent parameterization for dark energy (DE). We find that, if no priors are imposed on $\Omega_{0\rm m}$ and h, DE which evolves with time provides a better fit to the SNe data than ΛCDM. This is also true if we include results from the WMAP CMB data. From a joint analysis of SNe+CMB, the best-fit DE model has $w_0 \lesssim -1$ at the present epoch and the transition from deceleration to acceleration occurs at $z_T = 0.39 \pm 0.03$. However, DE evolution becomes weaker if the ΛCDM based CMB results $\Omega_{0\rm m} = 0.27 \pm 0.04$, $h = 0.71 \pm 0.06$ are incorporated in the analysis. In this case, $z_T = 0.57 \pm 0.07$. Our results also show that the extent of DE evolution is sensitive to the manner in which the supernova data is sampled.

1. Introduction

Supernova observations [1, 2] were the first to suggest that our universe is currently accelerating. Subsequently, a combination of results from cosmic microwave background (CMB) experiments and observations of galaxy clustering served to strengthen this world view [3, 4], and it is now believed that as much as 2/3 of the total density of the universe is in a form which has large negative pressure and which is usually referred to as dark energy (DE).

The earliest theoretical model of DE – the cosmological constant (Λ) – satisfied $w \equiv p/\rho = -1$. Since the energy density in Λ does not evolve, its present value $\rho_\Lambda \simeq 10^{-47}$ GeV^4 is also its initial value. As a result, the ratio ρ_Λ/ρ_r, where ρ_r is the radiation density, had the miniscule value 10^{-123} at the Planck time. The enormous amount of fine tuning this might involve led theorists to suggest that, like other forms of matter in the universe, DE density too may show significant time-evolution. However, this argument for significant variability of Λ with redshift is questionable. Actually, it is a variant of the Dirac's large number hypothesis that proved not to be valid in our Universe. For example, the density of water has also a miniscule value of 10^{-93} in Planck units (though, of course, larger than that of ρ_Λ), and we know that its relative change from present time up to redshifts of the order of one (due to possible variations of the fine structure constant and the electron and proton masses) is less than 10^{-5}. So, based

on the argument above, it would be wrong to assume that dark energy density should significantly change with redshift.

Another, more reliable reason to suggest a time dependent form of DE lies in the fact that our current accelerating epoch is unlikely to have been unique. In fact there is considerable evidence to suggest that the universe underwent an early inflationary epoch during which its expansion rapidly accelerated under the influence of an 'inflaton' field which, over sufficiently small time scales, had properties similar to those of a cosmological constant. Inspired by inflationary cosmology, quintessence models invoke a minimally coupled scalar field to construct a dynamically evolving model for DE.

Recent years have seen a flurry of activity in this area and there are currently, apart from quintessence, at least a dozen well motivated models of an accelerating universe in which dark energy is a dynamically evolving quantity (see reviews [5, 6, 7]). A simple categorization of DE models could be as follows:

(i) The cosmological constant, $w = -1$.

(ii) DE with w = constant $\neq -1$ (cosmic strings ($w = -1/3$), domain walls ($w = -2/3$). Quintessence with a sine hyperbolic potential [6]).

(iii) Dynamical DE, $w \neq$ constant. (Quintessence, Chaplygin gas [8], k-essence [9], braneworld models [10, 11, 12], etc.)

(iv) DE with $w < -1$. (scalar-tensor gravity models [13], phantom models, braneworld cosmology etc. [14, 15, 16, 17, 18].) ‡

In view of the large number of possibilities for DE it would not be without advantage to analyse the properties of DE in a model independent manner. Such an approach was adopted by Alam et al.[20] (henceforth Paper I) in which the Supernova data published by Tonry et al.[21] and Barris et al.[22] was analysed using a versatile ansatz for the Hubble parameter. Paper I discovered that dynamical DE fit the SNe observations better than ΛCDM and these results found support in the subsequent analysis of other teams [23, 24, 25, 26]. (Paper I referred to DE evolution as 'metamorphosis' since the DE equation of state appeared to metamorphose from a negative present value $w_0 \lesssim -1$ to $w \simeq 0$ at $z \simeq 1$.)

Recently Riess et al.[27] have reanalysed some earlier SNe data and also published new data relating to 16 type Ia supernovae discovered using the Hubble Space Telescope (HST). In the present paper we shall reconstruct the properties of DE using the new

‡ Note that the kinetic energy of the phantom scalar field is negative, thus phantom models are strongly unstable with respect to spontaneous creation of 4 particles: a particle-antiparticle pair of this scalar field and a particle-antiparticle pair of any usual matter quantum field (see [19] for the most recent investigation of this process). Scalar-tensor models of dark energy with the effective Brans-Dicke parameter $\omega > -3/2$ are free from this difficulty. However, a possible decrease of w below -1 in these models is typically of the order of $1/\omega$, and is therefore very small, as follows from Solar System tests of general relativity. In this context it is interesting that the Braneworld models suggested in [11] can give rise to an effective equation of state for dark energy which can be substantially less than -1, and yet not be plagued with any instabilities at the classical or quantum level.

SNe data set ('Gold' in [27]). We shall also use some of the CMB results obtained by WMAP in the later part of our analysis.

2. Reconstructing Dark Energy

Perhaps the simplest route to cosmological reconstruction is through the Hubble parameter, which in a spatially flat universe is related to the luminosity distance quite simply by [28, 29, 30]

$$H(z) = \left[\frac{d}{dz}\left(\frac{d_L(z)}{1+z}\right)\right]^{-1} . \tag{1}$$

We may now define the dark energy density as :

$$\rho_{\rm DE} = \rho_{0\rm c}\left[\left(\frac{H}{H_0}\right)^2 - \Omega_{0\rm m}(1+z)^3\right] , \tag{2}$$

where $\rho_{0\rm c} = 3H_0^2/(8\pi G)$ is the present day critical density of an FRW universe, and $\Omega_{0\rm m}$ is the present day matter density with respect to the critical density. However, one should keep in mind a subtle point regarding this definition of the dark energy density. Its ambiguity lies in the value of $\Omega_{0\rm m}$. From CMB and galaxy clustering data, we obtain an estimate of the total amount of clustered non-relativistic matter present today (denoted by $\tilde{\Omega}_{0\rm m}$). However, $\Omega_{0\rm m}$ may be *different* from $\tilde{\Omega}_{0\rm m}$ due to a contribution from a part of the unclustered dark energy which also has a dust-like equation of state. Fortunately, this difference (if it exists) appears to be small, e.g. not exceeding 0.1 for the best-fit shown in section (2.2).

Information extracted from SNe observations regarding $d_L(z)$ therefore translates directly into knowledge of $H(z)$, the dark energy density, and, through [31]

$$q(x) \;=\; -\frac{\ddot{a}}{aH^2} \equiv \frac{H'}{H}x - 1 , \tag{3}$$

$$w(x) = \frac{2q(x)-1}{3\,(1-\Omega_{\rm m}(x))} \equiv \frac{(2x/3)\;H'/H - 1}{1\;-\;(H_0/H)^2\Omega_{0\rm m}\;x^3}\;;\; x = 1+z , \tag{4}$$

into knowledge about the deceleration parameter of the universe and the equation of state of dark energy.

For a meaningful reconstruction of DE one must construct an ansatz for $H(z)$ which is sufficiently versatile to accommodate a large class of DE models. (Alternatively one could devise an ansatz for $d_L(z)$ or $w(z)$; for a summary of different approaches see [32, 20].) An ansatz which works quite well for Quintessence and also for the Chaplygin gas and Braneworld models is [33]

$$h(x) = \frac{H(x)}{H_0} = \left[\Omega_{0\rm m}x^3 + A_0 + A_1x + A_2x^2\right]^{\frac{1}{2}} \;,\; x = 1+z , \tag{5}$$

where $A_0 + A_1 + A_2 = 1 - \Omega_{0\rm m}$. Note that this ansatz should not be considered as a truncated Taylor series for $h^2(z)$. Rather, it is an interpolating fit for $h^2(z)$ having the right behaviour for small and large values of z. The number of terms in this fit is sufficient given the amount and accuracy of the present supernovae data. With more

and better data in future, more terms with intermediate (e.g., half-integer) powers of x may be added to it. Truncated Taylor series in powers of z with any finite number of terms may not be used to analyse most interesting quantities (including $h(z)$ and $d_L(z)$) for the already existing supernovae data since these series become divergent at $z \sim 1$. In particular, for the standard ΛCDM model ($A_1 = A_2 = 0$) the convergence radius of the Taylor expansions for $h(z)$ and $d_L(z)$ centered at $z = 0$ is given by the distance to the closest singular point in the complex z plane which lies at $z = (1/\Omega_{0\mathrm{m}} - 1)^{1/3} \exp(\pm i\pi/3) - 1$. So, for $\Omega_{0\mathrm{m}} = 0.3$ the Taylor series diverges at $z \geq 1.197$.

This is equivalent to the following ansatz for DE density (with respect to the critical density) :

$$\tilde{\rho}_{\mathrm{DE}}(x) = \rho_{\mathrm{DE}}/\rho_{0\mathrm{c}} = A_0 + A_1 x + A_2 x^2 \ , \tag{6}$$

which is exact for the cosmological constant $w = -1$ ($A_1 = A_2 = 0$) and for DE models with $w = -2/3$ ($A_0 = A_2 = 0$) and $w = -1/3$ ($A_0 = A_1 = 0$). Here, we neglect a possible difference between $\Omega_{0\mathrm{m}}$ and $\tilde{\Omega}_{0\mathrm{m}}$ mentioned above since it appears to be unimportant for the redshifts involved ($z < 2$), though it may become important for larger z.

The corresponding expression for the equation of state of DE is :

$$w(x) = -1 + \frac{A_1 x + 2A_2 x^2}{3(A_0 + A_1 x + A_2 x^2)} \ . \tag{7}$$

A glimpse into the properties of dark energy is also provided by a two parameter approximation for the equation of state :

$$w(z) = w_0 + w_1 \ z \ , \tag{8}$$

which can be trusted for small values of $z \lesssim 1$.

The likelihood for the parameters of the ansatz can be determined by minimising a χ^2-statistic:

$$\chi^2(H_0, \Omega_{0\mathrm{m}}, p_j) = \sum_i \frac{[\mu_{\mathrm{fit},i}(z_i; H_0, \Omega_{0\mathrm{m}}, p_j) - \mu_{0,i}]^2}{\sigma_i^2} \ , \tag{9}$$

where $\mu_{0,i} = m_B - M = 5\log d_L + 25$ is the extinction corrected distance modulus for SNe at redshift z_i, σ_i is the uncertainty in the individual distance moduli (including the uncertainty in galaxy redshifts due to a peculiar velocity of 400 km/s), and p_j are the parameters of the relevant ansatz (A_1, A_2 for the ansatz (5) and w_0, w_1 for the ansatz (8)). We assume a flat universe for our analysis but make no further assumptions on the nature of dark energy. For most of the following results, we marginalise over the nuisance parameter H_0 by integrating the probability density $\mathrm{e}^{-\chi^2/2}$ over all values of H_0.

We first study the different subsamples of the new SNe data reported in [27] in some detail using the ansatz (5) and (8). Riess et al.[27] reanalysed the existing SNe data compiled by different search teams (mainly the High Redshift Search Team (HZT) and the Supernova Cosmology Project (SCP) team) and added to these 16 new SNe

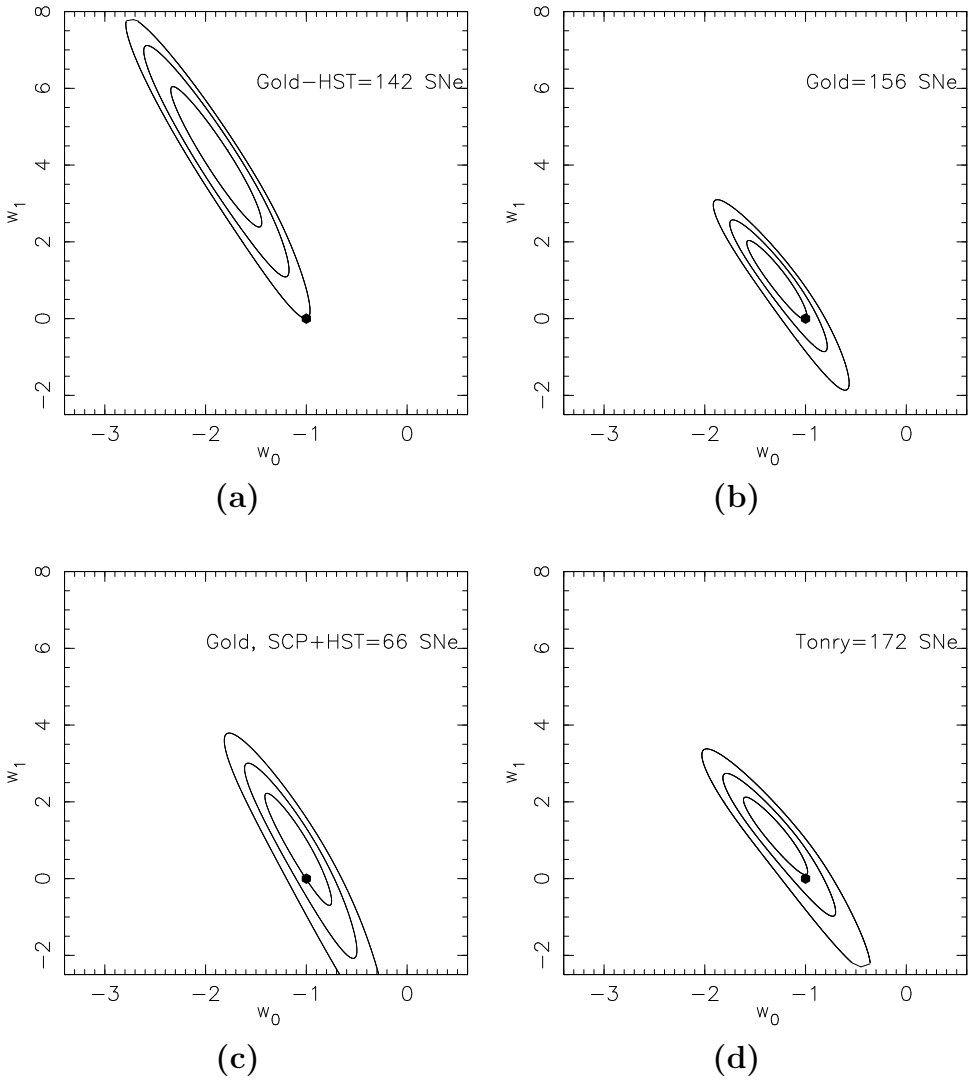

Figure 1. 1σ, 2σ, 3σ confidence levels in the $w_0 - w_1$ space for the ansatz (8) for $\Omega_{0\mathrm{m}} = 0.3$, using different subsets of data from [27]. The filled circle represents the ΛCDM point.

observed by HST. They have rejected many of the previously published SNe due to lack of complete photometric record, uncertain classification, etc. They divide the total data-set into "high-confidence" ('Gold') and "likely but not certain"('Silver') subsets. In our calculations we will consider their "high-confidence" ('Gold') subset. Figure 1 shows the (w_0, w_1) confidence levels for the ansatz (8) using different subsets of the new data for $\Omega_{0\mathrm{m}} = 0.3$. The top two panels in fig 1 are similar to the corresponding panels of figure 10 of [27], and the bottom panels show other subsets of data. The panel (a) shows the 'Gold' sample of [27] without the 14 new HST points, and the panel (b) shows the full 'Gold' sample of 156 SNe. Of the last two panels, the panel (c) shows the results for a subset of the 'Gold' sample, consisting only of the points obtained

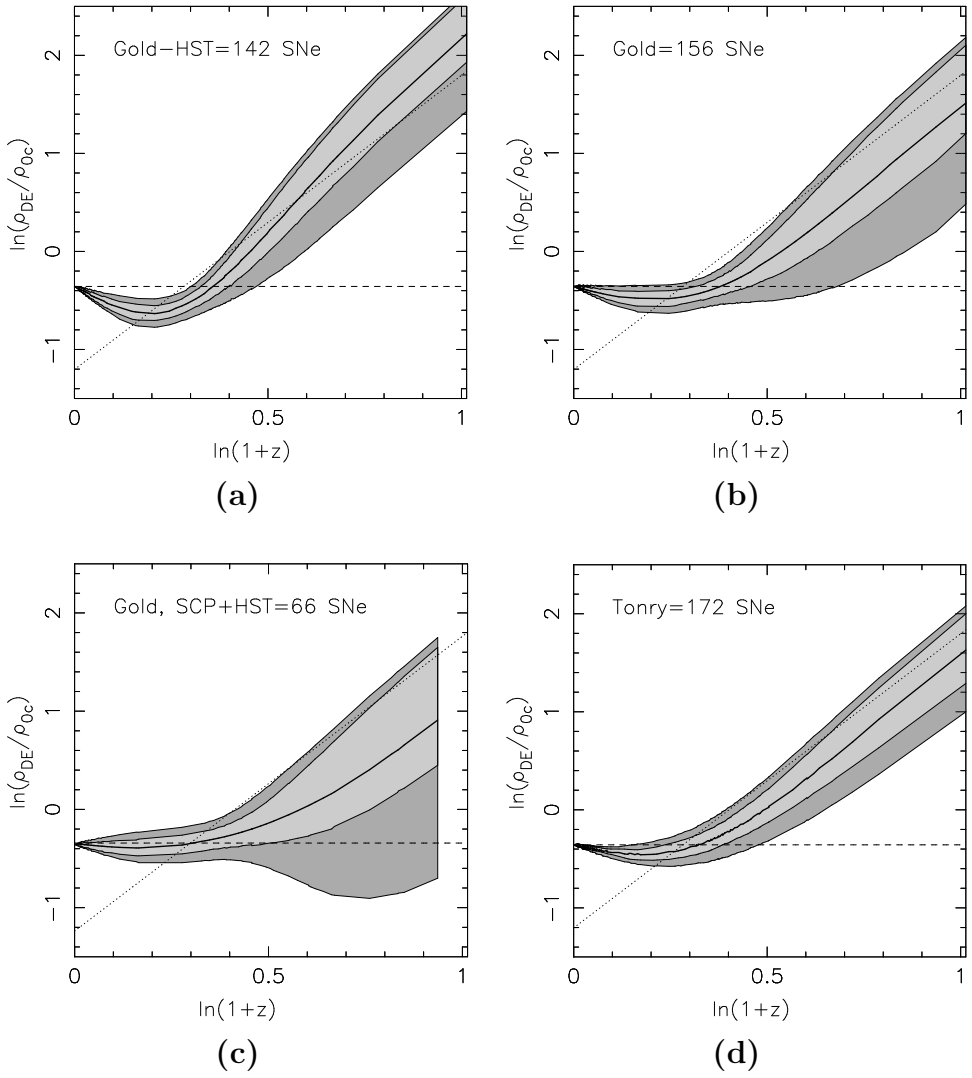

Figure 2. The logarithmic variation of dark energy density $\rho_{\rm DE}(z)/\rho_{0\rm c}$ (where $\rho_{0\rm c} = 3H_0^2/8\pi G$ is the present critical energy density) with redshift for $\Omega_{0\rm m} = 0.3$ using different subsets of data from [27], for the ansatz (5). In each panel, the thick solid line shows the best-fit, the light grey contour represents the 1σ confidence level, and the dark grey contour represents the 2σ confidence level around the best-fit. The dotted line denotes matter density $\Omega_{0\rm m}(1+z)^3$, and the dashed horizontal line denotes ΛCDM.

by the SCP team and the new HST points, while the panel (d) shows the confidence levels for the older data set of 172 SNe published in Tonry et al. [21]. The greatest difference is clearly between the panels (a) and (c). We should also note that the panel (b) (comprising of the new reanalysed data) and panel (d) (comprising of the old HZT data) are qualitatively similar, with panel (b) having tighter errors.

We now analyse these different subsets using the ansatz (5). In figures 2 and 3, we show the variation of dark energy density and dark energy equation of state obtained

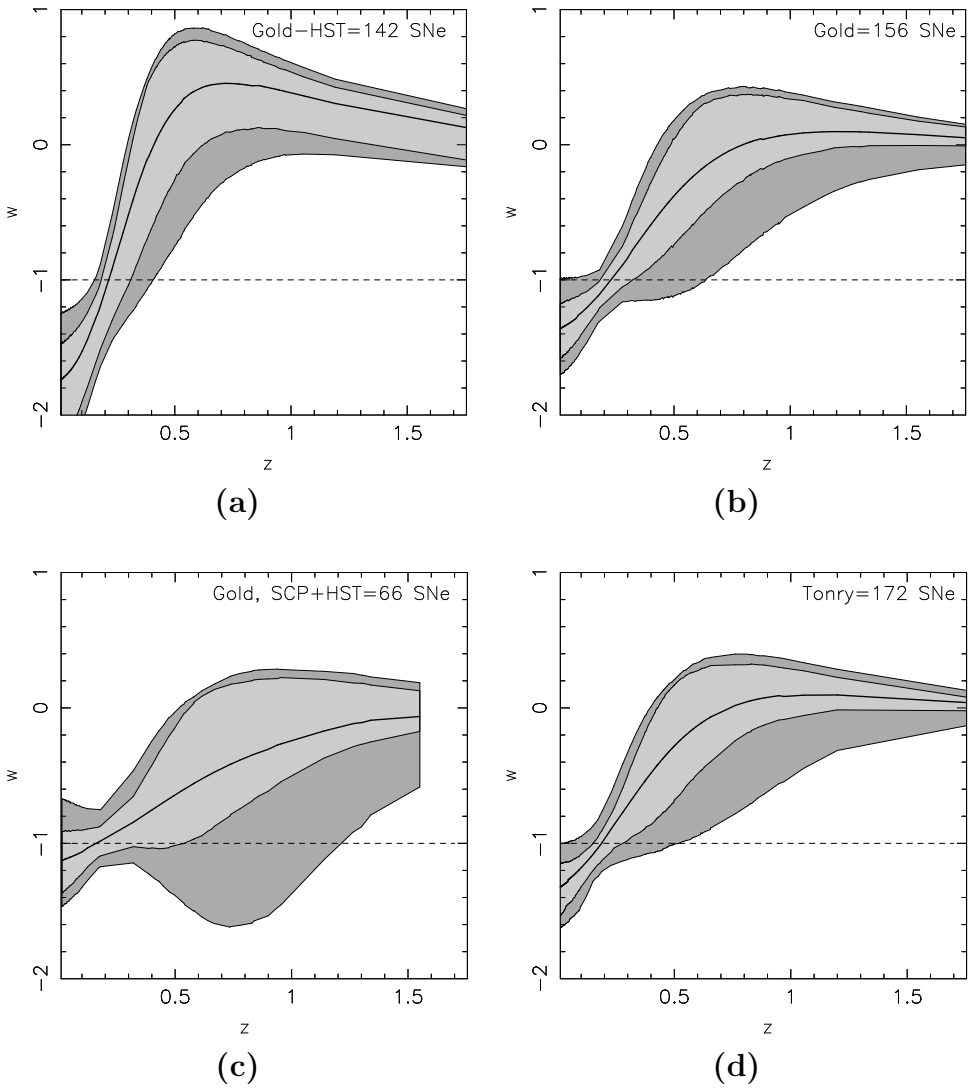

Figure 3. The variation of equation of state of dark energy $w(z)$ with redshift for $\Omega_{0\mathrm{m}} = 0.3$ using different subsets of data from [27], for the ansatz (5). In each panel, the thick solid line shows the best-fit, the light grey contour represents the 1σ confidence level, and the dark grey contour represents the 2σ confidence level around the best-fit. The dashed horizontal line denotes ΛCDM.

using the ansatz (5) for the different subsets of data, fixing $\Omega_{0\mathrm{m}} = 0.3$. It is interesting to note that panels (b) and (d) in both figures are quite similar, and we therefore conclude that the 'Gold' sample shows an evolution for DE which is consistent with that obtained from the older sample of Tonry et al.[21].

From figure 1 we find that for all four datasets, the largest degeneracy direction in $w_0 - w_1$ plane corresponds to the curve $w_0 + 0.25w_1 \simeq -1$. This immediately suggests that $w(z = 0.25) \simeq -1$, and this result appears to be quite robust since one can also arrive at it by choosing a very different ansatz (5) to determine $w(z)$, as shown in

figure 3.

As pointed out in [27], and confirmed by the figures 1, 2, 3, the *maximum evolution* in DE is for the 'Gold – HST' data. Less evolution is shown by the 'Gold' data set. However, we would like to emphasise again that the 'Gold' data set, which includes the 14 new HST points, gives roughly the same degree of evolution for DE as the original data reported in Tonry et al. [21] and analysed in [20]. Thus the results pertaining to the evolution of DE reported in Paper I remain valid also for the new SNe (Gold) data set.

Note that even the maximum rate of evolution of DE obtained in [20] in terms of w is $\frac{dw}{dz} \sim few$ which is in complete agreement with the results obtained in [27]. Does this mean however that the new supernovae data completely exclude models with a fast phase transition in dark energy [34, 35] for which $|\frac{dw}{dz}| \gg 1$ over a narrow range of redshift $\delta z \ll 1$? In our view such a conclusion would be premature. The reason is that using an ansatz such as (5) or (8) (as in [27]) is equivalent to smoothing the evolution of the Universe over a redshift interval $\Delta z \propto 1/N$, N being the number of free parameters used in the ansatz. Clearly, after such an implicit smoothing fast phase transitions in dark energy will disappear not so much because they disagree with the data but because of the manner in which the data has been analysed (see [20] for a more detailed discussion of these issues).

Figures 1, 2, and 3 also illustrate that the degree of DE evolution can be quite sensitive to the manner in which the SNe data is sampled. Comparing panels (a) and (c) in these figures, we find that the degree of evolution of DE is largest for the 'Gold – HST' data set and least for the 'Gold, SCP + HST' data. (The latter is in better agreement with ΛCDM than the other three data sets.)

2.1. Analysis of 'Gold' SNe dataset :

We now examine the 'Gold' data set in some detail using the polynomial expansion of dark energy, (5). In the figure 4 we show the confidence levels for the parameters (A_1, A_2) of the ansatz for three different values of $\Omega_{0\mathrm{m}}$. The χ^2 value for the best-fit in each case is given in table 1. The χ^2 values for the corresponding ΛCDM models are also given for comparison. Interestingly, in all three cases the confidence ellipse has the same inclination, it only appears to shift downwards as $\Omega_{0\mathrm{m}}$ increases.

In figure 5, we show the variation of the dark energy density with redshift for different values of the current matter density. We see that, for higher $\Omega_{0\mathrm{m}}$, the dark energy density evolution is sharper. The reader should also note that the growth of $\tilde{\rho}_{\mathrm{DE}}$ with time in the panels (b) and (c) is indicative of the phantom nature of DE ($w \leq -1$) at recent times ($z \lesssim 0.25$ for $\Omega_{0\mathrm{m}} = 0.3$ and $z \lesssim 0.4$ for $\Omega_{0\mathrm{m}} = 0.4$, see figure 6).

We may obtain more information from the dark energy density by considering a weighted average of the equation of state:

$$1 + \bar{w} = \frac{1}{\Delta \ln(1+z)} \int [1 + w(z)] d \ln(1+z) = \frac{1}{3} \frac{\Delta \ln \tilde{\rho}_{\mathrm{DE}}}{\Delta \ln(1+z)} \,, \qquad (10)$$

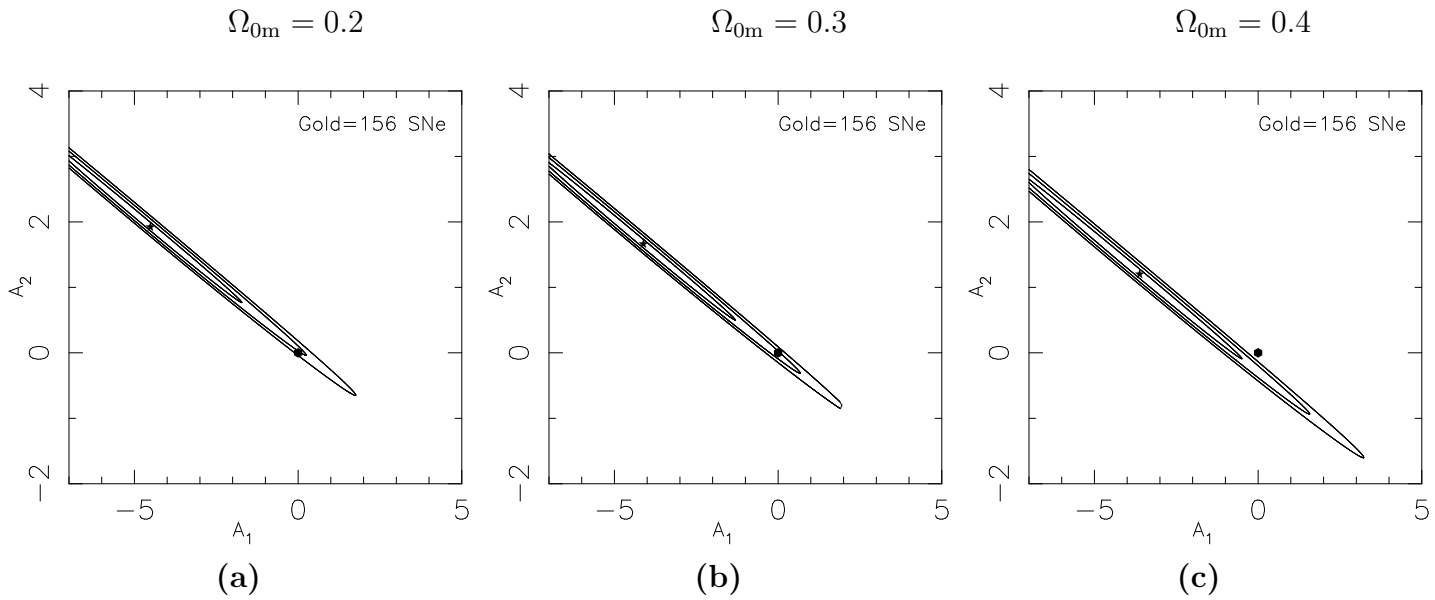

Figure 4. The (A_1, A_2) parameter space for the ansatz (5) for different values of Ω_{0m}, using the 'Gold' sample of SNe from [27]. The star in each panel marks the best-fit point, and the solid contours around it mark the $1\sigma, 2\sigma, 3\sigma$ confidence levels around it. The filled circle represents the ΛCDM point. The corresponding χ^2 for the best-fit points are given in table 1.

Table 1. χ^2 per degree of freedom for best-fit and ΛCDM models for analysis using the 'Gold' sample of SNe from [27]. w_0 is the present value of the equation of state of dark energy in best-fit models.

	Best-fit		ΛCDM
Ω_{0m}	w_0	χ^2_{min}	χ^2
0.20	−1.20	1.036	1.109
0.30	−1.35	1.034	1.053
0.40	−1.59	1.030	1.086

where Δ denotes the total change of the variable between integration limits. Thus the variation in the dark energy density depicted in figure 5 is very simply related to the weighted average equation of state of dark energy. The value of $\bar{w}$ for different ranges of integration are shown in table 2. We have taken the ranges of integration to be approximately equally spaced in $\ln(1+z)$. In all three cases shown, the value of $\bar{w}$ changes noticeably from close to -1 in the first bin to close to zero in the second bin. This indicates that the equation of state of DE is evolving from $w \lesssim -1$ today to $w \simeq 0$ at $z \simeq 1$. Note that these results are in very good agreement with those reported in Table 1 of Paper I.

Figure 6 shows the corresponding variation of the DE equation of state with redshift for different Ω_{0m}. Here also, there is strong evidence for evolution of DE. We see that

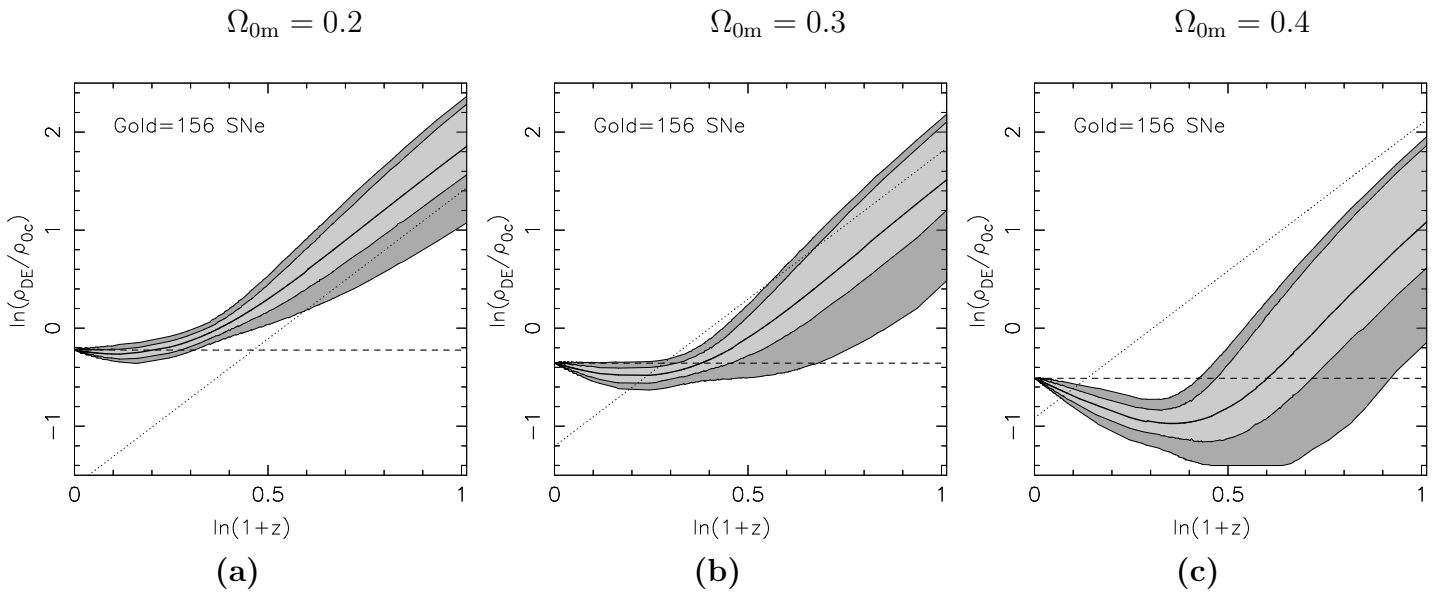

Figure 5. The logarithmic variation of dark energy density $\rho_{\rm DE}(z)/\rho_{0c}$ (where $\rho_{0c} = 3H_0^2/8\pi G$ is the present critical energy density) with redshift for different values of Ω_{0m}, using the 'Gold' sample of SNe from [27]. The reconstruction is done using the polynomial fit to dark energy, ansatz (5). In each panel, the thick solid line shows the best-fit, the light grey contour represents the 1σ confidence level, and the dark grey contour represents the 2σ confidence level around the best-fit. The dotted line denotes matter density $\Omega_{0m}(1+z)^3$, and the dashed horizontal line denotes ΛCDM.

Table 2. The weighted average $\bar{w}$ (eq 10) over specified redshift ranges for analysis using the 'Gold' sample of SNe from [27]. The best-fit value and 1σ deviations from the best-fit are shown.

	$\bar{w}$		
Ω_{0m}	$\Delta z = 0 - 0.414$	$\Delta z = 0.414 - 1$	$\Delta z = 1 - 1.755$
0.2	$-0.847^{+0.019}_{-0.043}$	$-0.118^{+0.280}_{-0.211}$	$0.089^{+0.067}_{-0.039}$
0.3	$-1.053^{+0.089}_{-0.070}$	$-0.159^{+0.319}_{-0.259}$	$0.118^{+0.073}_{-0.041}$
0.4	$-1.310^{+0.220}_{-0.179}$	$-0.210^{+0.452}_{-0.340}$	$0.215^{+0.081}_{-0.050}$

for higher values of Ω_{0m}, the dark energy equation of state has a more negative value at present and shows a sharper evolution over redshift. It is interesting to note that a constant equation of state which is < -1 during the evolution of the universe from $z \simeq 1.7$ to $z = 0$ appears not to be supported by the recent SNe data.

To summarize, our results clearly demonstrate that evolving DE is by no means excluded by the most recent SNe observations. On the contrary, our results for $\tilde{\rho}_{\rm DE}$ and $w_{\rm DE}$ obtained using the 'Gold' sample of [27] (figures 5, 6) are very similar to the results which we obtain using the SNe samples of [21, 22]. For $0.2 \leq \Omega_{0m} \leq 0.4$ the best-fit DE model evolves from $w \lesssim -1$ at $z \simeq 0$ to $w \simeq 0$ at $z \simeq 1$ in agreement with the results

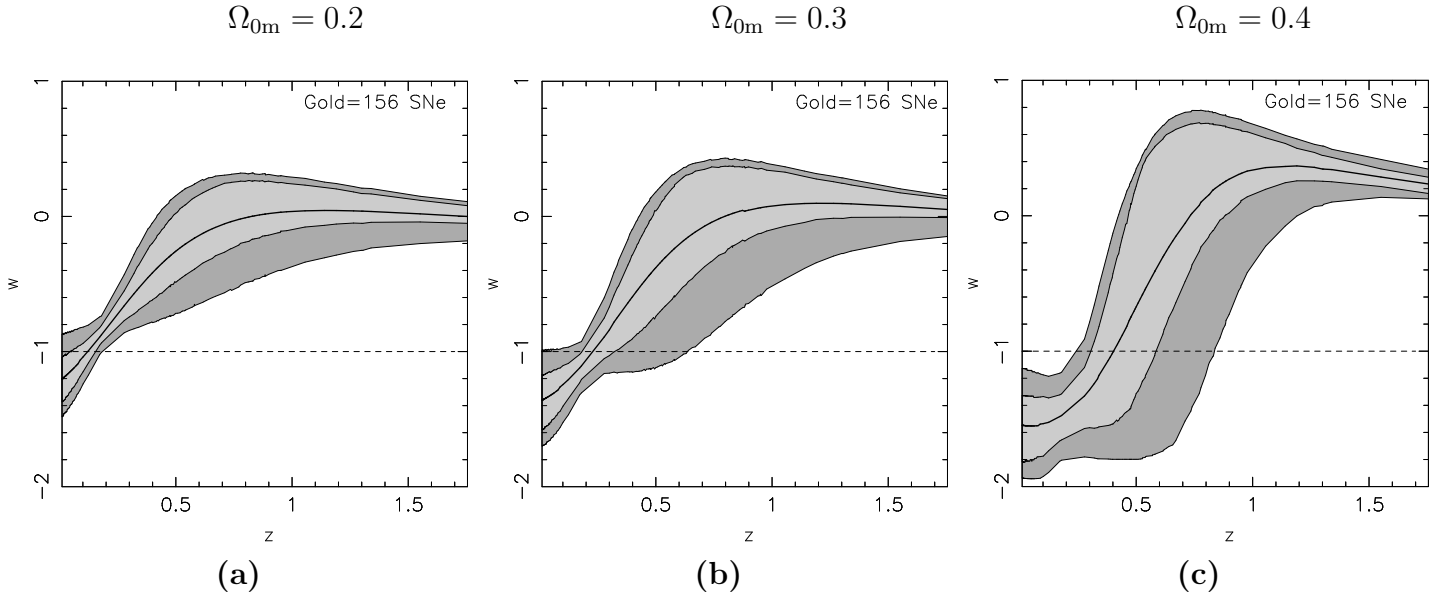

Figure 6. The evolution of $w(z)$ with redshift for different values of $\Omega_{0\mathrm{m}}$, for the 'Gold' sample of SNe from [27]. The reconstruction is done using the polynomial fit to dark energy, equation (5). In each panel, the thick solid line shows the best-fit, the light grey contour represents the 1σ confidence level, and the dark grey contour represents the 2σ confidence level around the best-fit. The dashed line represents ΛCDM.

of Paper I.

2.2. DE reconstruction using SNe('Gold')+CMB :

Observations of the cosmic microwave background and Type Ia supernovae provide us with complementary insight into the nature of dark energy [36, 37, 38, 39]. We may use the WMAP result of $R = \sqrt{\Omega_{0\mathrm{m}}}\int_0^{z_{\mathrm{ls}}} dz/h(z) = 1.710 \pm 0.137$ (from WMAP data alone) in conjunction with the SNe 'Gold' sample to reconstruct DE. For this purpose, we use $\Omega_b h^2 = 0.024$ and $\Omega_{0\mathrm{m}} h^2 = 0.14 \pm 0.02$ [3]. To calculate z_{ls} we use a fitting function given in [40]:

$$z_{ls} = 1048[1 + 0.00124(\Omega_b h^2)^{-0.738}][1 + g_1(\Omega_{0\mathrm{m}} h^2)^{g_2}] \ , \tag{11}$$

where

$$g_1 = 0.078(\Omega_b h^2)^{-0.238}[1 + 39.5(\Omega_b h^2)^{0.763}]^{-1}, \tag{12}$$

$$g_2 = 0.56[1 + 21.1(\Omega_b h^2)^{1.81}]^{-1} \ . \tag{13}$$

Figure 7 shows our reconstruction of DE obtained with the ansatz (5) using the WMAP result together with the SNe 'Gold' sample. The best fit values for this reconstruction are: $\Omega_{0\mathrm{m}} = 0.385, A_1 = -2.87, A_2 = 1.01, h = 0.60$. The best fit dark energy density is $\tilde{\rho}_{\mathrm{DE}}(x) = 2.475 - 2.87x + 1.01x^2$. Note that the best fit $\tilde{\rho}_{\mathrm{DE}}$ decreases monotonically with redshift up to $z \simeq 0.4$ and then begins to increase. This reflects the

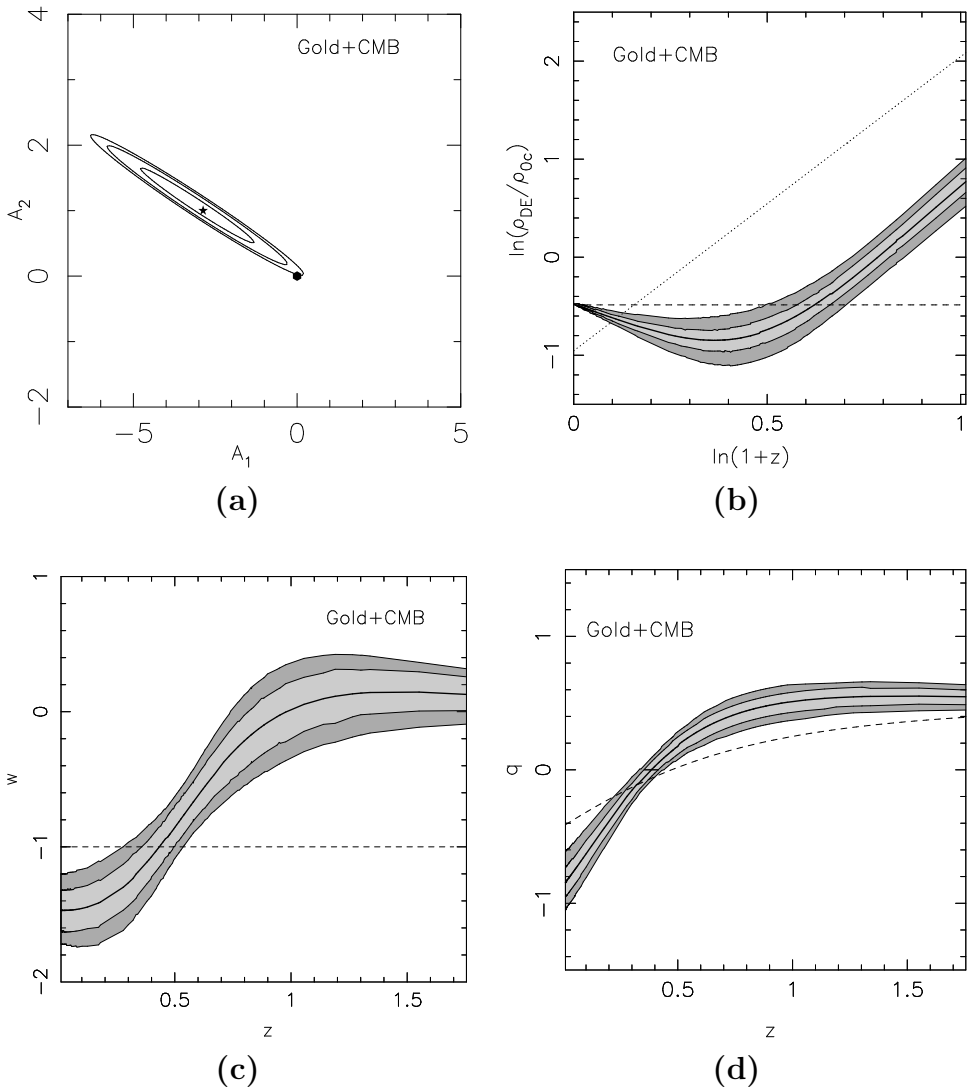

Figure 7. Results from analysis of SNe(Gold)+CMB data, using ansatz (5). $\Omega_{0\mathrm{m}}$ and h are fixed at best-fit values of $\Omega_{0\mathrm{m}} = 0.385, h = 0.60$. Panel (a) shows the confidence levels in the (A_1, A_2) parameter space. The star marks the best-fit and the filled circle marks the ΛCDM point. Panel (b) shows the logarithmic variation of dark energy density with redshift. Panel (c) shows the evolution of dark energy equation of state with redshift. Panel (d) shows the variation of the deceleration parameter with redshift. In all three panels (b), (c) and (d), the thick solid line represents the best-fit, the light grey contours represent the 1σ confidence level, and the dark grey contours represent the 2σ confidence levels. The dashed line in panels (b), (c) and (d) represents ΛCDM, and the dotted line in panel (b) represents the matter density. The horizontal thick solid line in (d) represents the 1σ limits on the transition redshift at which the universe starts accelerating.

Table 3. The weighted average $\bar{w}$ (eq 10) over specified redshift ranges for analysis from SNe+CMB data. The best-fit value and 1σ deviations from the best-fit are shown.

	$\bar{w}$		
$\Omega_{0\mathrm{m}}$	$\Delta z = 0 - 0.414$	$\Delta z = 0.414 - 1$	$\Delta z = 1 - 1.755$
0.385	$-1.287^{+0.016}_{-0.056}$	$-0.229^{+0.070}_{-0.177}$	$0.142^{+0.051}_{-0.033}$

phantom nature of DE ($w < -1$) at lower redshifts. The equation of state behaves as before, evolving from $w_0 \lesssim -1$ to $w \simeq 0$ at $z \simeq 1$. From the figure 7(d), we see that the deceleration parameter q has a value of $q_0 = -0.84 \pm 0.11$ at present. The transition from deceleration to acceleration ($q(z_T) = 0$)occurs at a redshift of $z_T = 0.39 \pm 0.03$. Therefore, from a joint analysis of CMB and SNe data, one may obtain a fairly good idea of when the universe began to accelerate. These results demonstrate that the best fit to SNe+CMB observations favours evolving DE with a somewhat higher value of $\Omega_{0\mathrm{m}}$ and a slightly lower value of h. Note that the value of $\Omega_{0\mathrm{m}}$ is larger than the WMAP result $\Omega_{0\mathrm{m}} = 0.27 \pm 0.04$ obtained using the ΛCDM prior, but is in agreement with the results obtained in [41, 42] ($\Omega_{0\mathrm{m}} \simeq 0.35 \pm 0.12$) using high redshift clusters. Also note that, because of the dust-like behaviour of DE at higher redshifts, the above value of $\Omega_{0\mathrm{m}}$ obtained using equations (2-5) maybe somewhat larger than the values obtained for $\Omega_{0\mathrm{m}}$ from clustering measurements. The value of $h \simeq 0.60$ obtained for the best fit is in tension with the ΛCDM based result from WMAP, $h = 0.73 \pm 0.03$, but is in agreement with the observations of [43, 44, 45, 46, 47, 48, 49] which can accommodate lower values of $h \sim 0.6$ (see also the discussion in [50] in this context). We therefore conclude that a joint analysis of SNe and CMB data favours evolving DE over ΛCDM if no priors are placed on $\Omega_{0\mathrm{m}}$ and h separately ($\Omega_{0\mathrm{m}}h^2 = 0.14 \pm 0.02$ is assumed).

It is however a useful exercise to see how the behaviour of DE would change if strong priors were imposed on $\Omega_{0\mathrm{m}}$ and h. We therefore show results obtained by using the ΛCDM based CMB priors [3]: $\Omega_{0\mathrm{m}} = 0.27 \pm 0.04$ and $h = 0.71 \pm 0.06$. The best fit in this case has $\Omega_{0\mathrm{m}} = 0.29$ and a dark energy density of $\tilde{\rho}_{\mathrm{DE}} = 1.23 - 0.81x + 0.29x^2$. The equation of state at present is $w_0 = -1.10$, and it slowly evolves to $w(z = 1.75) \simeq -0.4$. The deceleration parameter has a value of $q_0 = -0.63 \pm 0.12$ at present and the redshift at which the universe begins to accelerate is $z_T = 0.57 \pm 0.07$. Figure 8 demonstrates that the time evolution of DE is *extremely weak* in this case and is in good agreement with ΛCDM cosmology (see also [51]).

3. Conclusions

In conclusion, we find that the case for evolving dark energy (originally demonstrated in Paper I) is upheld by the new supernova data if no priors are imposed on $\Omega_{0\mathrm{m}}$ and h. For a reasonable range of $0.2 \leq \Omega_{0\mathrm{m}} \leq 0.4$, the equation of state of dark energy evolves from $w_0 < -1$ today to $w_0 \simeq 0$ at $z \simeq 1$. The above result remains in place if we add CMB

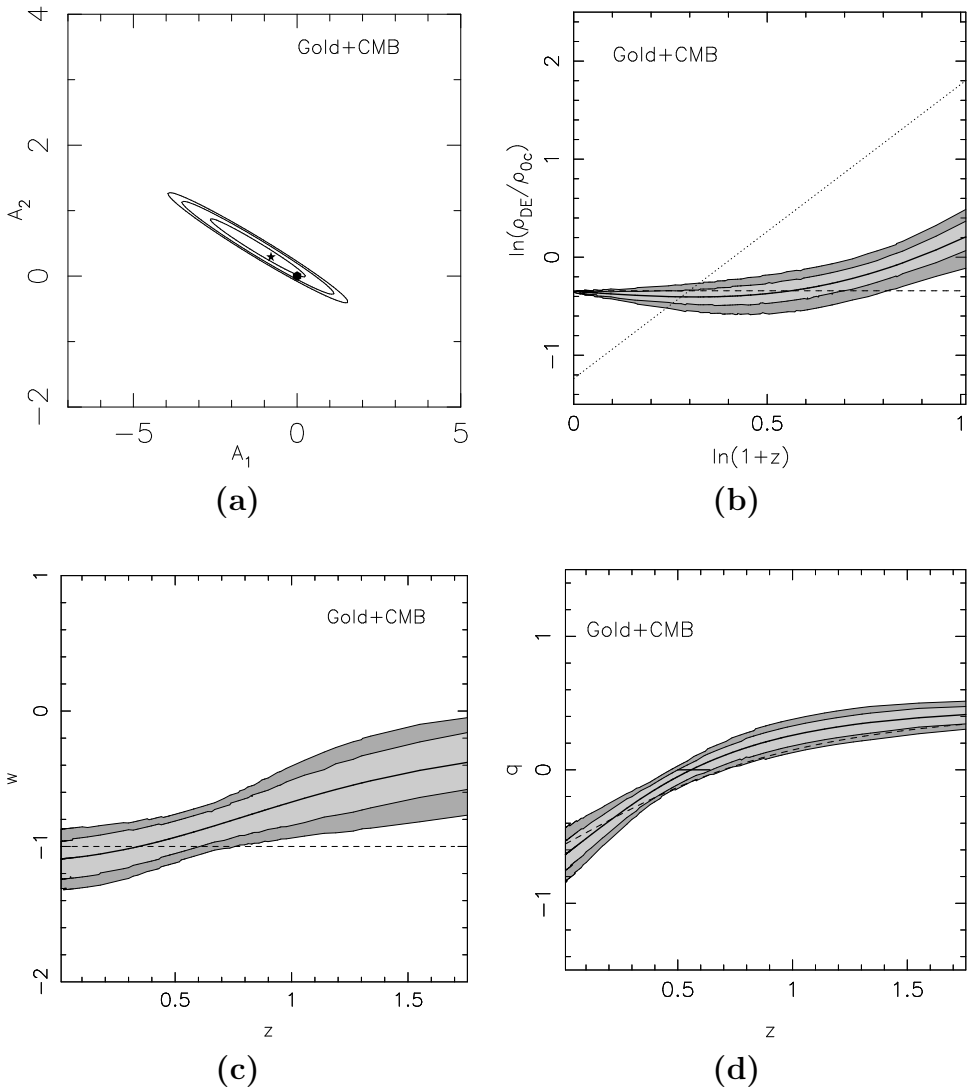

Figure 8. Results for analysis of SNe(Gold)+CMB data with ΛCDM-based WMAP priors of $\Omega_{0\mathrm{m}} = 0.27 \pm 0.04$ and $h = 0.71 \pm 0.06$, using ansatz (5). Panel (a) shows the confidence levels in the (A_1, A_2) space. The star marks the best-fit and the filled circle marks the ΛCDM point. Panel (b) shows the logarithmic variation of dark energy density with redshift. Panel (c) shows the evolution of dark energy equation of state with redshift. Panel (d) shows the variation of the deceleration parameter with redshift. In all three panels (b), (c) and (d), the thick solid line represents the best-fit, the light grey contours represent the 1σ confidence level, and the dark grey contours represent the 2σ confidence levels. The dashed line in panels (b), (c) and (d) represents ΛCDM, and the dotted line in panel (b) represents the matter density. The horizontal thick solid line in (d) represents the 1σ limits on the transition redshift at which the universe starts accelerating.

priors to the analysis. In this case, evolving dark energy with $\Omega_{0\mathrm{m}} \simeq 0.385$ and $h \simeq 0.6$ is favoured over ΛCDM, and the epoch at which the universe began to accelerate is $z_T = 0.39 \pm 0.03$ within 1σ. However, if we assume strong priors on $\Omega_{0\mathrm{m}}$ and h using the ΛCDM based WMAP results, then the best-fit chooses an $\Omega_{0\mathrm{m}} = 0.29$. The evolution in the equation of state becomes weaker and is in much better agreement with ΛCDM. The redshift of transition from deceleration to acceleration is $z_T = 0.57 \pm 0.07$, which is closer to the ΛCDM value of $z_T \simeq 0.7$ for this value of $\Omega_{0\mathrm{m}}$. Finally, one must note that the DE evolution becomes weaker or stronger depending on the subsampling of the SNe dataset. A larger number of supernovae at high redshifts, as well as better knowledge of the values of H_0 and $\Omega_{0\mathrm{m}}$ are therefore required before firm conclusions are drawn about the nature of dark energy.

4. Acknowledgements

We would like to thank Arman Shafieloo for useful discussions. UA thanks the CSIR for providing support for this work. AS was partially supported by the Russian Foundation for Basic Research, grant 02-02-16817, and by the Research Program "Astronomy" of the Russian Academy of Sciences.

References

[1] Riess A et al., 1998 Astron. J. **116** 1009 [astro-ph/9805201]
[2] Perlmutter S J et al., 1999 Astroph. J. **517** 565 [arXiv:astro-ph/9812133]
[3] Spergel D N et al., 2003 Astroph. J. Suppl. **148** 175 [astro-ph/0302209]
[4] Tegmark M et al., 2004 Astroph. J. **606** 702 [astro-ph/0310725]
[5] Sahni V, 2002 Class. Quantum Grav. **19** 3435 [astro-ph/0202076]
[6] Sahni V and Starobinsky A A, 2000 Int. J. Mod. Phys. **D9** 373 [astro-ph/9904398]
[7] Sahni V, 2004 astro-ph/0403324
[8] Kamenshchik A, Moschella U and Pasquier V, 2001 Phys. Lett. B **511** 265
[9] Armendariz-Picon C, Mukhanov V and Steinhardt P J, 2000 Phys. Rev. Lett. **85** 4438 [astro-ph/0004134]
[10] Deffayet C, Dvali G and Gabadadze G, 2002 Phys. Rev. D **65** 044023 [astro-ph/0105068]
[11] Sahni V and Shtanov Yu V, 2003 JCAP **0311** 014 [astro-ph/0202346]
[12] Alam U and Sahni V, 2002 astro-ph/0209443
[13] Boisseau B, Esposito-Farese G, Polarski D and Starobinsky A A, 2000 Phys. Rev. Lett. **85** 2236 [gr-qc/0001066]
[14] Caldwell R R, 2002 Phys. Lett. B **545** 23 [astro-ph/9908168]
[15] McInnes B, 2002 JHEP **0208** 029 [hep-th/0112066]
[16] Caldwell R R, Kamionkowski M and Weinberg N N, 2003 Phys. Rev. Lett. **91** 071301 [astro-ph/0302506]
[17] Carroll S M, Hoffman M and Trodden M, 2003 Phys. Rev. D **68** 023509 [astro-ph/0301273]
[18] Melchiorri A, Mersini L, Odman C J and Trodden M, 2003 Phys. Rev. D **68** 043509 [astro-ph/0211522]
[19] Cline J M, Jeon S y and Moore G D, 2003 hep-ph/0311312
[20] Alam U, Sahni V, Saini T D and Starobinsky A A, 2003 astro-ph/0311364
[21] Tonry J L et al., 2003, Astroph. J. **594** 1 [astro-ph/0305008]
[22] B. J. Barris et al., 2004, Astroph. J. **602** 571B [astro-ph/0310843]

[23] Wang Y and Mukherjee P, 2004, Astroph. J. **606** 654 [astro-ph/0312192]
[24] Nesseris S and Perivolaroupolos L, 2004 astro-ph/0401556
[25] Gong Y, 2004 astro-ph/0401207
[26] Daly R A and Djorgovski S G, 2004 astro-ph/0403664
[27] A. G. Riess et al., 2004 Astroph. J. **607** 665 [astro-ph/0402512]
[28] Starobinsky A A, 1998 JETP Lett. **68** 757 [astro-ph/9810431]
[29] Huterer D and Turner M S, 1999 Phys. Rev. D **60** 081301 [astro-ph/9808133]
[30] Nakamura T and Chiba T, 1999 Mon. Not. Roy. Ast. Soc. **306** 696 [astro-ph/9810447]
[31] Saini T D, Raychaudhury S, Sahni V and Starobinsky A A, 2000 Phys. Rev. Lett. **85** 1162 [astro-ph/9910231]
[32] Alam U, Sahni V, Saini T D and Starobinsky A A, 2003 Mon. Not. Roy. Ast. Soc. **344** 1057 [astro-ph/0303009]
[33] Sahni V, Saini T D, Starobinsky A A and Alam U, 2003 JETP Lett. **77** 201 [astro-ph/0201498]
[34] Bassett B A, Kunz M, Silk J and Ungarelli C, 2002, Mon. Not. Roy. Ast. Soc. **336** 1217 [astro-ph/0203383]
[35] Corasaniti P S, Bassett B A, Ungarelli C and Copeland E J, 2003, Phys. Rev. Lett. **90** 091303 [astro-ph/0210209]
[36] Bond J R, Efstathiou G and Tegmark M, 1997 Mon. Not. Roy. Ast. Soc. **291** L33 [astro-ph/9702100]
[37] Doran M, Lilley M, Schwindt J and Wetterich C, 2001 Astroph. J. 559 501 [astro-ph/0012139]
[38] Bean R and Melchiorri A, 2002 Phys. Rev. D **65** 041302 [astro-ph/0110472]
[39] Hu W, Fukugita M, Zaldarriaga M, Tegmark M, 2001 Astroph. J. **549** 669 [astro-ph/0006436]
[40] Hu W and Sugiyama N, 1996 Astroph. J. **471** 30 [astro-ph/9510117]
[41] Schueker P, Caldwell R R, Bohringer H, Collins C A and Guzzo L, 2003 Astron. Astrophys. **398** 867 [astro-ph/0208251]
[42] Borgani S et al., 2001 Astroph. J. **561** 13 [astro-ph/0106428]
[43] Saha A et al., 1997 Astroph. J. **486** 1
[44] Tammann G A, Sandage A and Reindl B, 2003 Astron. Astrophys. **404** 423 [astro-ph/0303378]
[45] Allen P D and Shanks T, 2004 Mon. Not. Roy. Ast. Soc. **347** 1011A [astro-ph/0102447]
[46] Freedman W L et al., 2001 Astroph. J. **553** 47 [astro-ph/0012376]
[47] Battistelli E S et al., 2003 Astroph. J. **598** L75 [astro-ph/0303587]
[48] Reese E D et al., 2002 Astroph. J. **581** 53 [astro-ph/0205350]
[49] Mason B S, Myers S T and Readhead A C, 2001 Astroph. J. **555** L11 [astro-ph/0101169]
[50] Conversi L, Melchiorri A, Mersini L and Silk J, 2004 astro-ph/0402529
[51] Wang Y and Tegmark M, 2004 astro-ph/0403292